Analytical and numerical studies of mass flux dispersed from tapered swirl atomizer with various nozzle cut profiles

IOP Conf. Series: Materials Science and Engineering **610** (2019) 012040 doi:10.1088/1757-899X/610/1/012040

Analytical and numerical studies of mass flux dispersed from tapered swirl atomizer with various nozzle cut profiles

Hatem Kayed

Mechanical Power Engineering Department, Cairo University, Egypt

E-mail. hatem_kayed@yahoo.com

Abstract. Spraying dispersed fluid by swirl atomizer into a main gas stream in order to obtain homogeneous blended flow within a restricted distance from the atomizer position is a significant issue. The dispersal of sprayed fluid mass-flux from the atomizer should be correlated to mass flux distribution of the main flow gas. Consequently, it is essential to control the distribution of liquid mass flux from the injector to match the distribution of main gas flux to attain perfect mixing with identical liquid/gas mass flux ratio all over the pipe. The present study examines the liquid mass flux pattern injected from tapered swirl atomizer having various cut shapes. A mathematical approach to circumferentially evaluate the outlet mass fraction distribution from generalized tapered nozzle cut was analyzed. The derived mass fraction distribution equation is dependent on the flow-angle, the cut-angle, and the arc-angle. A CFD simulation was performed to evaluate the flow angle at the outlet from the nozzle cut. The finding of the present work delivers a guide for researchers and engineers to the preferred injector cut profile to give the best mass flux uniformity. The simulated spray pattern relied on circumferential mass flux at nozzle outlet has been in great coincidence with what depicted by imaging. More studies could be performed to have the most appropriate cut shape of the injector with various flow profiles of the main gas stream.

1. Introduction

Swirl atomizer is utilized in numerous applications because of its superior atomization with lesser energy in respect to other regularly utilized pressure atomizers. The swirling movement made by the swirler in the atomizer prompts a centrifugal force that drives the sprayed fluid to shape a film connected to the outlet nozzle-wall and issuing a low-pressure internal air core [1]. As the film leaves the outlet nozzle, it gives a uniform spread of mass flux and establishes a hollow cone shape of spray for a flat-cut profile. An investigation to evaluate the film-thickness and the shape for a flat cut spout was already analyzed [2]. One of the serious issues of the flat-cut swirl atomizer is the susceptibility of varying spray dimension and geometry with the surrounding circumstances and the nozzle end temperature [3]. Earlier research [4] demonstrated that for a nozzle-cut with a constant angle lower than the flow-angle prompts a hollow-cone injection shape without worsening the atomization characteristics. The work demonstrated likewise that the cut-angle can principally influence the mass spread over the periphery of the nozzle. In this way, to create an open-side spray pattern, a prior determination of the flow-angle is essential.

The Flow-angle α is expressed as the angle between the exit flow velocity from the nozzle and its axis. The angle is chiefly constrained by the swirler configuration and the nozzle length. The flow-angle could be postulated equivalent to 0.5 of the spray angle [1,5]. In an additional analysis [6], it was discovered that the estimated flow-angle is corrected with a factor of 0.6315. The evaluation study for

the flow close to the outlet tip discovered that the opening-angle of the spray rises till it achieves an asymptotic number that equivalent to the spray-angle [3]. The spray-angle, in this way, relies upon droplet penetration from the nozzle tip. The study demonstrated that film-thickness, differential pressure, and Weber number are influencing the spray-angle [2]. Various measurement techniques were performed to estimate the flow-angle, the least difficult technique is the utilization of direct-imaging with extensive exposure time [3]. Another technique utilizes fluorescence PIV method [7]. The flow-angle could likewise be evaluated numerically as long as the nozzle configuration and dimensions are identified. Single and two-phase flow analysis was performed in the literature [8].

Though the vast majority of the aforementioned work has been carried out for gasoline-direct injectors, a pressure swirl atomizer can be utilized in numerous industrial usages: spray drying, agriculture, metal powder and fire suppression [5]. One of these usages require mounting the injector on the pipe surface to provide a liquid spray into the main gas stream to obtain uniform blend within a narrow span from the injector, for instance: spraying Urea inside the exhaust-pipe of internal combustion engines to lower NOx [9]. Because of the short distance between the catalyst and the exhaust manifold, Urea must be sprayed and efficiently blended with the main exhaust stream within this short distance before entering the catalytic converter. The application of mixer to perform this job makes a boosting in engine back-pressure causing power deficiency whereas, mounting swirl injector with an optimized cut profile at nozzle exit can help in enhancement in uniformity of Urea and exhaust stream within this short distance without any flow obstruction or blockage.

In the present work, an analytical correlation was derived to obtain the distribution of mass-flux emerged from any cut-angle of the nozzle. The analytical results were validated by images and mass-flux measurements obtained from employing mechanical-patternator.

2. Analytical Methodology

It was postulated that flow velocity at nozzle exit is uniform. Furthermore, the film-thickness at nozzle exit was kept constant as well across the cut profile. The scope of the present section is to set up an analytical approach to evaluate the distribution of mass-flux from a general nozzle cut profile. It was postulated that the flow velocity at the nozzle exit is uniform. Furthermore, the film-thickness at nozzle exit was kept constant as well across the cut profile. Based on the principle analysis done by Moon et al. [4], an analytical approach was developed to evaluate the volume-fraction besides, the produced injection pattern at a generalized cut shape. Figure 1 presents a basic cut shape having an angle γ. Height y can be expressed in terms of x as:

$$y = f(x) = x \,.\, \tan(\gamma) \tag{1}$$

To recognize this derivation, the cut-angle nozzle having a cut-angle γ has been unfolded and projected, see Figure 2.

$$x = r.\,(1 - \cos(\theta)) \tag{2}$$

$$y(\theta) = r \,.\, \tan(\gamma).\,(1 - \cos(\theta)) \tag{3}$$

the following assumptions are considered:

- Constant sheet thickness across tapper-cut circumference.
- Uniform and constant flow-angle, $(90 - \alpha)$ across tapper-cut circumference.
- Uniform axial and peripheral speeds across tapper-cut circumference.

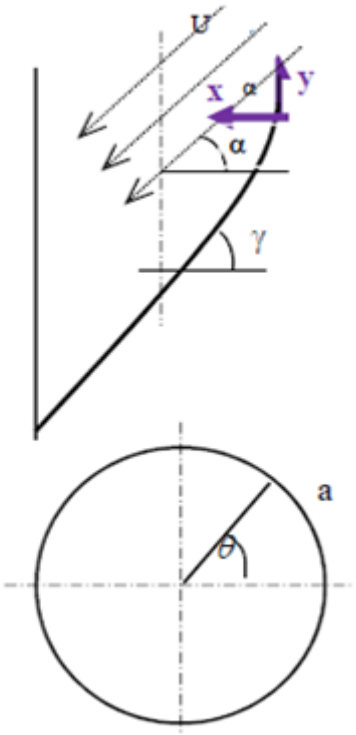

Figure 1: Sectional view of flow direction having angle α inside nozzle cut of angle ɣ

The surface slope tan (ϕ) at any angle (θ) can be expressed as:
To estimate the exit mass flow from nozzle, the normal velocity is U_f is calculated as follows (see figure 2).

$$tan(\phi) = \frac{1}{r} \cdot \frac{dy}{d\theta} = tan(\gamma) \cdot sin(\theta) \quad (4)$$

To estimate the exit mass flow from nozzle, the normal velocity is U_f is calculated as follows (see figure 2).

$$U_f = U.\, sin(\alpha - \phi) \quad (5)$$

where U is the absolute flow velocity and α is the flow angle

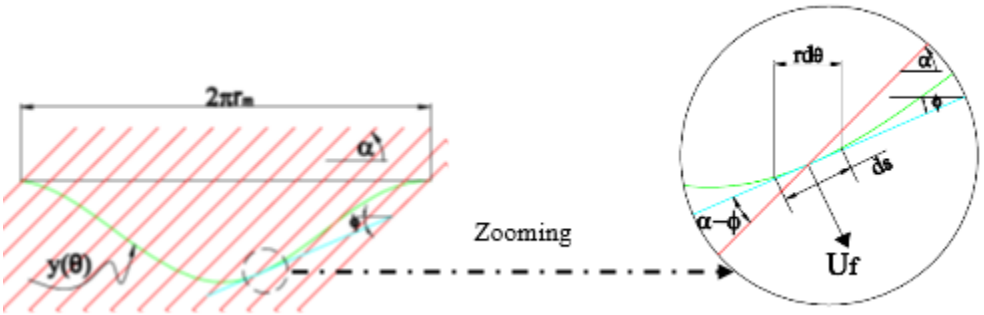

Figure 2: Projection of tapered cut at nozzle exit illustrating main angles, dimensions and normal velocity direction

The outlet discharge flow-rate is expressed as;

$$dV = U_f . ds \tag{6}$$

The outlet area is identified as;

$$ds = \frac{r\, d\theta}{\cos(\Phi)} . h \tag{7}$$

From eq (5) and (7), exit volume flow rate across dθ is as

$$dV = u_f . ds = \mathrm{U} . \sin(\alpha - \Phi) . \frac{r. d\theta}{\cos(\Phi)} . h \tag{8}$$

By applying simple trigonometry analysis, $\sin(\alpha - \Phi) = \sin(\alpha) . \cos(\Phi) - \cos(\alpha) . \sin(\Phi)$, substituting into Eq. (5) and reformulating;

$$dV = r . h . u . d\theta . [\sin(\alpha) - \cos(\alpha) . \tan(\gamma) . \sin(\theta)] \tag{9}$$

The exit mass fraction can be expressed as;

$$\frac{dm}{m_t} = \left[1 - \frac{\tan(\gamma)}{\tan(\alpha)} . \sin(\theta)\right] . \frac{d\theta}{2\pi} \tag{10}$$

Obviously, with increasing the cut-angle, the amount of outlet spray decreases till having a critical value at which no mass issuing from the nozzle, that corresponds to ($\phi = \alpha$). When the flow-angle, α, approaches ϕ, the liquid flow in the nozzle transports in the same line with the tapper cut slope without issuing outflow from the nozzle [10].

If ($\phi > \alpha$), the injection outflow begins to form without any liquid spray between θ_1 and θ_2 (see Figure 3).

At $\Phi = \alpha$, $tan(\Phi) = tan(\alpha)$, substituting into eq (4)

$$sin\ \theta_1 = \frac{tan(\alpha)}{tan(\gamma)} \tag{11}$$

From figure 3, the straight line relation presents that

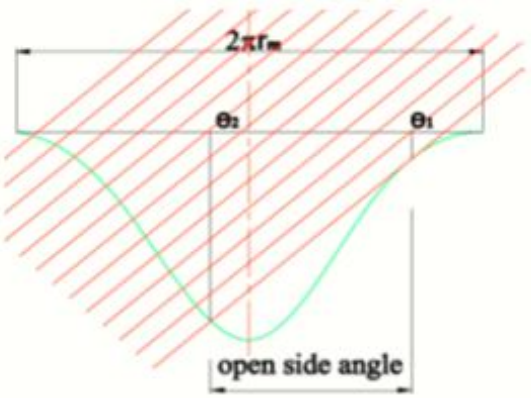

Figure 3: Illustration of open angle across Δθ

$$\frac{y_2 - y_1}{r. (\theta_2 - \theta_1)} = tan(\alpha) \tag{12}$$

$$y_2 - y_1 = r . (\theta_2 - \theta_1) . tan(\alpha) \tag{13}$$

$$r . \tan(\gamma) . (1 - cos(\theta_2)) - r . \tan(\gamma) . (1 - \cos(\theta_1)) = r . (\theta_2 - \theta_1) . tan(\alpha) \tag{14}$$

$$\theta_1 - \theta_2 + \frac{\tan(\gamma)}{tan\,(\alpha)}(cos(\theta_1) - \cos(\theta_2)) = 0 \quad (15)$$

As a result of the assumptions involved, there are slight differences between the predicted results obtained from the present analysis and what are reported in other work employing fan spray analysis [11].

Eq. *(10)* could be reformulated to be in general form for any cut shape, *y = f (x)*.

$$\frac{dm}{m_t} = \left[1 - \frac{\bar{y}' \,.\, sin(\theta)}{\tan(\alpha)}\right] . \frac{d\theta}{2\pi} \quad (16)$$

where $\bar{y}' = \frac{d\bar{y}}{d\bar{x}}\Big|_{x=0.5(1-\cos\theta)}$ $\bar{y} = y/D$, $\bar{x} = x/D$

The mass fraction exiting from notch cut injector case, equation (16) yields to;

$$\frac{dm}{m_t} = \left[1 - \frac{\bar{y}'}{\tan(\alpha)} \,.\, sin(\theta + k)\right] . \frac{d\theta}{2\pi} \quad (17)$$

k = π at θ = (π/2 to 3π/2), otherwise *k = 0*;

The general position at which the injection begins to spray from $\theta_1$to θ_2 occurs when (Φ ≥ α). Where θ_1 ,θ_2 could be calculated as follows;

$$sin\,(\theta_1) = \frac{\bar{y}'}{tan(\alpha)} \quad (18)$$

$$\theta_1 - \theta_2 + \frac{\bar{y}'}{tan\,(\alpha)}(cos(\theta_1) - cos(\theta_2 + \mathrm{k})) = 0 \quad (19)$$

3. Spray Simulation

To validate the results of the previous analytical approach, a swirl injector was designed and fabricated from Acrylic as presented in Figure 4 where water stream was supplied at various pressures. The injector is with 4 tangential openings situated inside the packaging body that creates the whirling movement (see Fig. 5). A cut of 70° from horizontal axis was chosen for the present case study. A trial was performed to estimate the injected mass flow by using manual patternator that has eight thin hoses distributed uniformly as presented in Figure 6. A flow simulation inside the injector was carried out utilizing STAR CCM+ CFD. Steady isothermal turbulent flow case was solved. RNG k-ε turbulence model was adopted because it is very simple and robust [11]. Non-uniform meshing technique with very smaller meshes close to wall boundary was utilized. A CFD analysis was performed for predicting the tilting of flow with respect to the horizontal axis, "flow angle".

Figure 4: Acrylic sprayer showing the outlet hole of cut-angle 70°

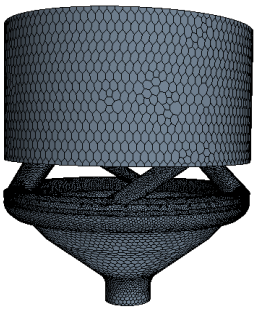

Figure 5. Mesh generation in the injector

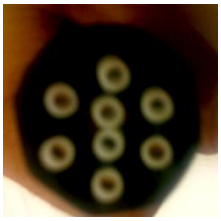

Figure 6: Mechanical patternator of eight tubes

4. Discussion of results

The upcoming sections present the numerical and experimental results, showing the spray images and flow simulation. In addition, the distribution of mass flux for tapered and notch nozzle cuts at various angles was presented and discussed.

4.1 Imaging and Simulation of Spray

The objective of the experimental work done is to validate the analytical results. In spite of the fact that this case study was previously attempted for gasoline direct injection (GDI) [4], it was reinvestigated here by utilizing water at lower injection pressures to prove the general expression that has been analyzed previously. Figure 7 presents the basic tulip pattern that is developed at lower injection pressure at cut-angle of 70^o. Additional rise to injection pressure brings the developed pattern of spray which is presented in figure 8. Imaging the spray from a different view, shows that the spray is injected from one side however, no-flow is injected from the other opposite side as depicted in figure 9. From image analysis, the spray cone angle was assessed to be 60^o for such injector.

Figure 7: typical tulip shape of the spray at a low injection pressure

Figure 8: Frontal view of the fully developed spray

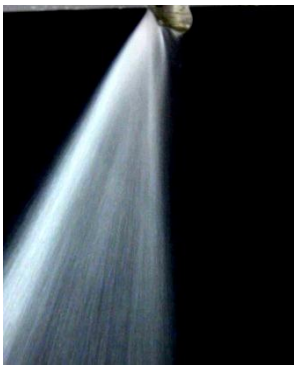

Figure 9: Side view of the fully developed spray

As concluded in many works of literature [1,5], the flow-angle was postulated to be 0.5 of spray cone-angle. When applying this conclusion to the present case study, the flow-angle will be 30^o. However, CFD simulations over predict such value and its estimation differs according to the calculation technique adopted. Weight-averaged technique estimates a value of 49^o, whereas using the maximum peripheral & axial velocities to estimate the flow-angle showed a value of 47^o. If the correction to flow-angle was utilized by multiplying it by 0.6315 as reported in [6] to estimate the half of spray cone-angle, it brings a value of 29.6^o for 49^o and 30.9^o for 47^o which agrees with the measured spray cone-angle. The flow-angle value is underestimated when using single-phase modeling when compared with two-phase modeling [11]. Figure 10 presents the streamlines of swirling flow motion inside the nozzle and the velocity vectors at its exit.

As shown from figure 11, the spray mass fluxes issued from nozzle cut-angles 30^o, 50^o and 70^o are represented at 30^o flow-angle. Figure 12 shows the comparison between the circumferential distribution of injected mass-fraction, dm/dm_t, at the three nozzle cut-angles. It demonstrates unequal outlet mass-fraction along the nozzle perimeter. It is observed that increasing the cut-angle leads to uneven distribution, increasing mass flux from the certain side while decreasing it in the opposite side, up to approaching a condition at which no outflow exits across a portion of nozzle circumference. These findings have been observed in the shots taken for the present Acrylic injector (see figure 8), besides they were recently confirmed with the results of gasoline direct swirl sprayer. It is significant to report the variation of cross-sectional area and normal velocity across the nozzle circumference. Figure 13 presents the symmetrical distribution of the cross-section area with θ. In spite of the fact that the zones are identical across both axes (see Fig. 13). However, normalized speeds show an asymmetric

distribution with θ (see Fig.14). The normal velocity is very low in the upper half (θ= 0º to 180º), while it is very high in the bottom half (θ= 180º to 360º). The case of 70º cut-angle shows that no outflow mass for certain circumference portion of the nozzle.

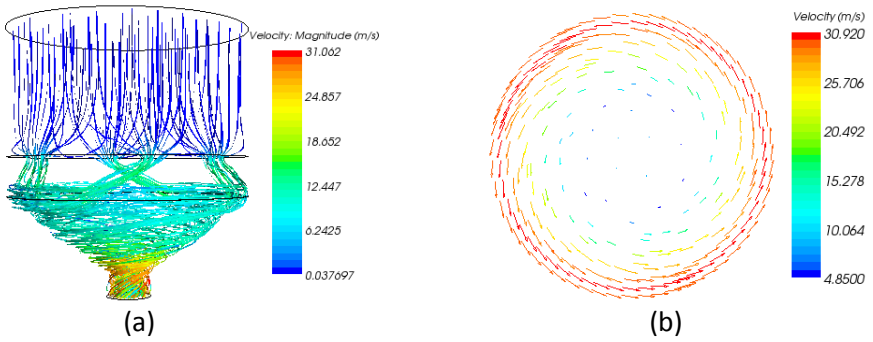

Figure 10: (a) Streamlines inside a swirling chamber, (b) velocity vectors inside the outlet nozzle exit

4.2 Spray distributions for a tapered-nozzle cut

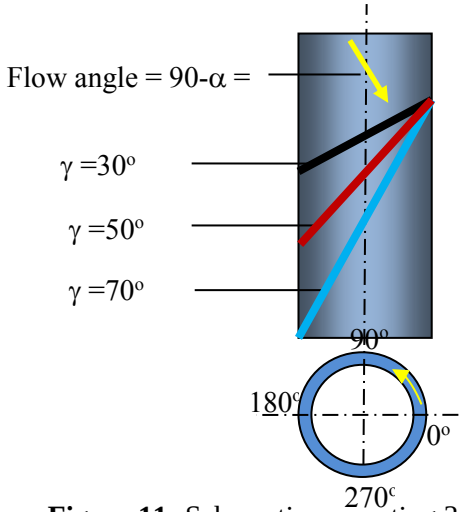

Figure 11: Schematic presenting 3 fixed nozzle cut-angles

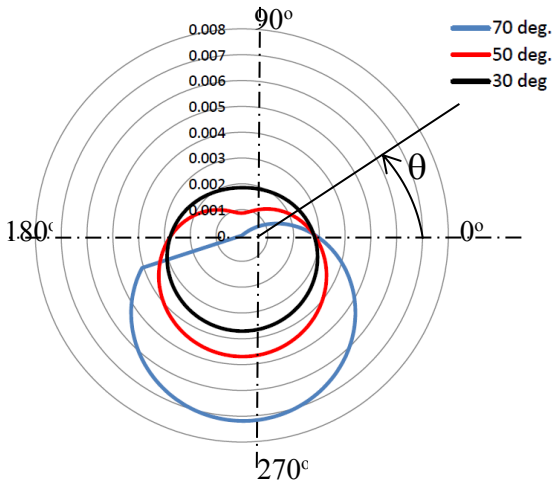

Figure 12: Distribution of mass-fraction with θ for 3 nozzle cut-angles

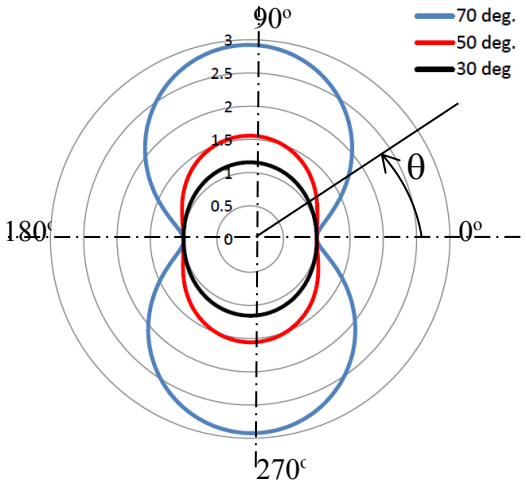

Figure 13: Variation of normalized arc area with θ for 3 nozzle cut-angles

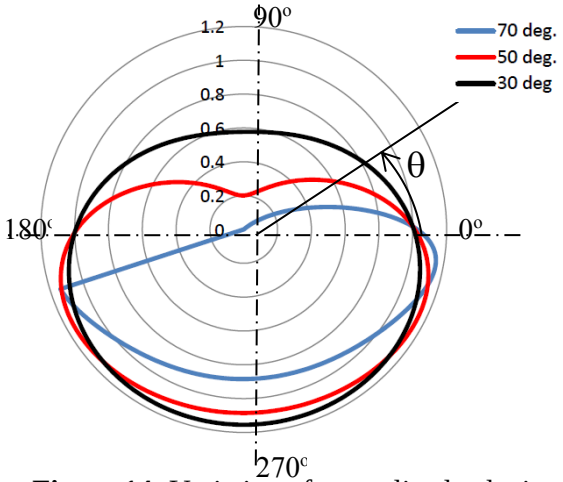

Figure 14: Variation of normalized velocity with θ for 3 nozzle cut-angles

4.3 Spray distributions for a notched-nozzle cut

The same analysis was taken place for 3 notched-nozzle cuts of various angles 30º, 50º, and 70º as displayed in Figure 15. The variation of mass fraction distribution, dm/dm_t, across the circumference with θ is presented in figure 16. Each distribution is symmetrical, having mass fraction flux over the whole range of θ with the cut-angles 30º and 50º, however, for the case of 70º, there is no outflow mass flux across a portion of nozzle circumference. This outflow portion increases with increasing cut angles above 70º. Figure 17 demonstrates the variation of normalized cross-sectional versus θ, which shows symmetrical distribution around both horizontal and vertical axes. The distribution of normal velocity indicates identical profiles for all cut-angles of notched nozzle injector as depicted in figure 18. The case of 70º cut-angle shows that no outflow mass with no normal velocity for certain circumference portion of the nozzle.

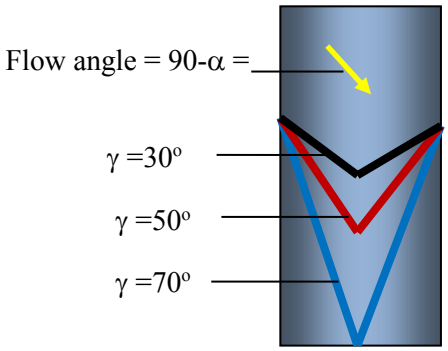

Figure 15: Schematic presenting 3 notched-nozzle cuts

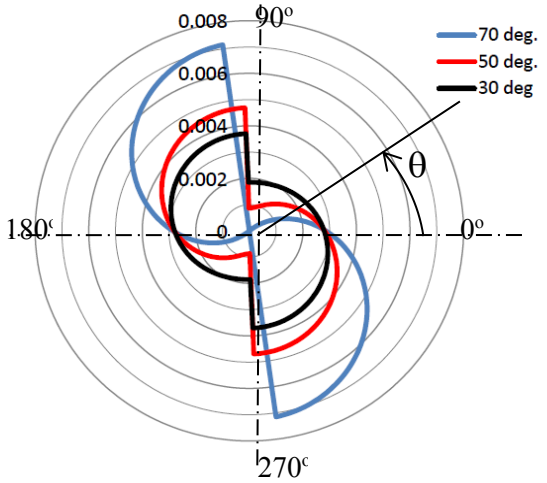

Figure 16: Distribution of mass-fraction with θ for 3 cut-angles of notched nozzle injector

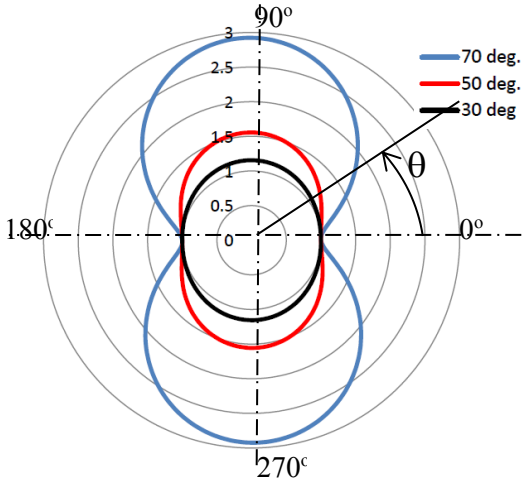

Figure 17: Variation of normalized arc area with θ for 3 nozzle cut-angles of the notched nozzle

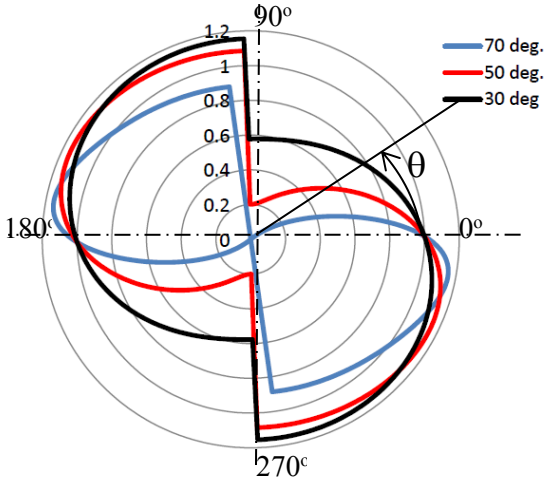

Figure 18: Variation of normalized velocity with θ for 3 nozzle cut-angles of the notched nozzle

5. Conclusions

An analytical approach was carried out to estimate the general distribution of mass fraction spray across nozzle circumference of any cut shape; y = f(x). The outcomes indicate different spray patterns can be developed with uneven distribution of outlet mass flux. The present study investigated 2 case studies, one of the tapered-cut profile while the other of notched-cut. The predicted spray pattern of the tapered nozzle cut has been achieved by imaging the spray shape issued from the Acrylic injector (locally manufactured). Despite the fact that the present analysis obtains the various distributions of mass flux with various spray patterns depending on the nozzle cut profile, but the engineer should choose the appropriate cut profile which fits the application purpose. The study demonstrated that various spray patterns can be issued according to cut-shapes, hence there is a great availability to produce the best spray pattern that matches the main gas stream distribution. This matching helps to obtain the optimum mixing performance in many challenging practices.

References

[1] Ren, W. M. and Nally Jr, J. F., "Computations of Hollow-Cone Sprays from a Pressure-swirl Injector" Society of Automotive Engineering SAE 982610, (1998)
[2] Moon, S, Bae, C, and Abo-Serie, E. F., "Estimation of the breakup length for a pressure-swirl spray from the experimentally measured spray angle" Atomization and Sprays 3: 235-246 (2009)
[3] VanDerWege, B. and Hochgreb, S., "Effects of Fuel Volatility and Operating Conditions on Fuel Sprays in DISI Engines: (1) Imaging Investigation," Society of Automotive Engineering, SAE 2000-01-0536, (2000)
[4] Moon, S.,Abo-Serie, E. F. and Bae, C., "The spray characteristics of a pressure-swirl injector with various exit plane tilts" International Journal of Multiphase Flow, 7: 615-627 (2008)
[5] Lefebvre, A. H. Atomization and Sprays, Hemisphere publishing corporation, 1989
[6] Cousin, J. and Nuglisch, " Modeling of internal flow in high pressure swirl injectors", SAE Transactions European Conference on Liquid Atomization and Spray Systems,Toulouse, France, July, 1999
[7] Khoo, Y. C. and Hargrave, G. K., "Real-Sized Pressure Swirl GDI Injector Investigation with HSFV and FPIV" Journal of Physics: Conference Series 45: 77–84, (2006)
[8] Kubo, M., Sakakida, A. and Iiyama, A., "Technique for Analyzing Swirl Injectors of Direct Injection Gasoline Engines" Society of Automotive Engineering, 2001-01-0964, (2001)
[9] Johansson, A., Wallin, U., Karlsson, M, Isaksson, A. And Bush, P., "Investigation on Uniformity Indices Used for Diesel Exhaust Aftertreatment Systems" Society of Automotive Engineering, SAE 2008-01-0613, (2008)
[10] Abdel Aziz, F. "CFD Simulation of Fuel Spray Patterns from Tapered Swirl Injector inside an Air-Flow Pipe" MSc thesis, Cairo University, (2013).
[11] Ren, W. M., Shen, J. And Nalley Jr, J. F." Geometrical Effects Flow Characteristics of a Gasoline High Pressure Swirl Injector" Society of Automotive Engineering SAE 971641, (1997)